Novel Laser-Based Deposition of Active Protein Thin Films

B.R. Ringeisen*, J. Callahan, P. Wu§, A. Pique, B. Spargo, R.A. McGill, M. Bucaro, H. Kim, D.M. Bubb, and D.B. Chrisey

Naval Research Laboratory, Code 6372, Washington DC 20375

§ *Permanent Address: Department of Physics, Southern Oregon University, Ashland OR 97520.*

**Corresponding Author: tel (202)404-2096, fax (202)767-5301, email: ringeisn@ccs.nrl.navy.mil*

Abstract

This paper reports the deposition of active protein thin films by a novel laser-based approach termed matrix assisted pulsed laser evaporation (MAPLE). We have deposited uniform 10 nm to nearly 1 ìm thin films of insulin and horseradish peroxidase (HRP). We performed several experiments to characterize the chemical integrity of the deposited films. Matrix assisted laser desorption/ionization (MALDI) and liquid chromatography/electrospray ionization mass spectrometry (LC/ESIMS) experiments performed on MAPLE-deposited insulin films indicate the laser-material interaction involved in this deposition technique does not modify the protein's mass. Fourier transform infrared spectroscopy (FTIR) experiments show that the chemical functionality and secondary structure of MAPLE-deposited HRP is nearly identical to the native protein. We also find that deposited HRP films retain their ability to catalyze the reduction of 3,3'-diaminobenzidine (DAB), suggesting that the active site of transferred proteins is unaffected by the MAPLE process. We also produced patterns and multilayers with feature sizes from 20 to 250 ìm by depositing different biomaterials through a shadow mask. Patterns of physisorbed HRP were then protected from dissolution in aqueous environment by a semi-permeable, polymer overlayer that was deposited *in situ* using pulsed laser deposition (PLD). This polymer membrane protects the protein pattern when it is exposed to DAB solution and enables the optical observation of HRP activity for spots as small as 2000 ìm^2. These results demonstrate that MAPLE is a preferred technique for depositing active biomolecules for applications ranging from microfluidic sensor devices to gene and protein recognition microarrays.

Introduction

Versatile methods for forming thin films of proteins, antibodies, and DNA are necessary to fulfill needs in next-generation applications such as microfluidic biosensors

and biochips, gene and protein recognition microarrays, coatings to prevent device failure due to biofouling, and biocompatible coatings for medical implants and implantable devices.[1,2,3,4,5,6,7,8,9,10,11,12,13] These applications each have different parameters for thin films and often place specific constraints on the techniques used to deposit them. For example, DNA or antibody microarrays require hundreds to thousands of different biomolecules to be placed adjacently and within tens of microns.[4,5,6,7,8] A prosthetic joint may require a single coating or multilayers of biomaterials that are continuous (uniform) and well adherent to reduce inflammation, decrease friction and wear (lubrication), or increase its biocompatibility.[3,10,11,12,13] Microfluidic devices for detecting biological or environmental analytes may require different proteins, enzymes, or cells to be patterned and immobilized adjacently, with varying film thicknesses, and with micron resolution.[1,2] These devices will also require coatings to enhance biocompatibility or to prevent device failure due to biofouling or contamination.[3,9] This manuscript describes a novel laser-based method to vapor deposit films and patterns of active proteins that has the potential to meet many of these next generation requirements.

Current technologies for depositing thin films and patterns of biomolecules are numerous and can be grouped into two categories: 1) techniques that pattern monolayers (or slightly thicker multilayer films), and 2) techniques that form patterns of thicker films (> 500 nm). Langmuir-Blodgett dip coating using self-assembled monolayers (SAM's) is the most common method to functionalize surfaces with single biomolecular layers.[14,15] In conjunction with other technologies, such as photo- and soft lithography, this technique can be used to form patterns of various biomolecules including proteins.[16,17,18] Film thickness can also be controlled by forming multilayers, but increasing the thickness

requires repeating the coating procedure for each additional layer and is limited in the materials used to create the film (typically amphiphiles). Soft lithography is a term that encompasses a group of relatively new techniques that use micromachined polymer stamps and SAM technology to transfer patterns of biomolecules to more adhesive substrates.[1,19,20] One of these approaches is termed microcontact printing (ìCP). This technique has excellent pattern resolution (pattern width < 1 ìm) and the ability to form patterns of proteins and other biomaterials, but it is generally used to deposit monolayer films and requires repeated stamping to form multiple layers.[21,22] Other techniques are capable of patterning proteins by using microfluidic channels to confine the flow of solutions containing the molecule of interest.[23,24,25] By exposing biomaterials in this manner to an adhesive substrate, adjacent patterns of different biologicals, including cells, can be formed.[26]

There are also several techniques capable of forming patterns of thicker biomaterial films. Several researchers have shown that ink jet printing is able to deposit films and patterns of biomolecules for a range of commercial applications.[27,28,29] By using multiple print heads, this technique is capable of producing adjacent patterns of different biomaterials, although jet clogging is problematic when multiple materials with different chemical and physical properties are deposited. Ink jet processes are able to produce spots less than 30 ìm in diameter, but cannot produce near-monolayer coverage and thickness control is dependent on the size of the dispensed droplet and surface wetting. There are also laser-based direct write technologies that show promise as novel techniques to form mesoscopic patterns of biomaterials. One such technique dispenses biomaterials by utilizing a laser to guide proteins and cells down a hollow fiber,[30,31] while

another approach uses a UV laser pulse to forward transfer active proteins and viable cells from a solid support to a receiving substrate.[32]

Attempts have also been made to form thin films of proteins through conventional laser-based deposition processes. In 1990 Nelson, *et al*. demonstrated that DNA molecules could be transferred from a frozen aqueous target intact by using pulsed laser energy.[33] This approach, termed matrix assisted laser desorption/ionization time-of-flight (MALDI-TOF), embeds a biomaterial in a matrix to shield it from damage by the incident laser. The ionized biomaterial is then directed into a time-of-flight tube for energy and mass analysis. Tsuboi et al. used a laser ablation deposition technique to deposit silk fibroin from a solid target to quartz and ZnSe substrates in vacuum.[34] The infrared spectrum of the deposited material was nearly identical to the bulk, pressed target material, but a mass distribution of the deposited material was not reported. Phadke et al. used a variation of this technique to form films of bacteriorhodhopsin and glucose oxidase.[35,36] In order to reduce the laser interaction with the protein, a composite target was formed containing the protein in a surfactant matrix. The surfactant was found to protect the biomaterial, and films of active protein were formed. This approach, however, results in a contaminant-rich film that contains not only the protein of interest but also the surfactant used in the target.

Here we describe the formation of pure biomolecular films by a novel laser-based deposition technique termed matrix assisted pulsed laser evaporation (MAPLE). MAPLE was originally developed as a psuedo-dry method to produce high quality films of chemo-selective polymers.[37,38,39] It is an attempt to avoid the pitfalls found in solvent-based coating technologies such as inhomogeneous films, inaccurate placement of

material, and difficult or inaccurate thickness control. MAPLE is an extension of pulsed laser deposition (PLD), which often is unable to successfully form films of complex polymers or biomolecules due to the irreversible photo-initiated destruction of chemical bonds required for desorption. MAPLE is able to avoid this damage by embedding a polymer or biomolecule in a UV-absorbent, high vapor pressure solvent. The resulting matrix preferentially absorbs the incident laser energy and the collective action of multiple collisions of the evaporating solvent with the embedded molecule result in a soft desorption with excellent structural fidelity. This approach has been shown to successfully form homogeneous films of several chemo-selective polymers.[38]

In this work, we successfully used the MAPLE technique to deposit thin films of biomolecules with excellent control over surface morphology and thickness (10 nm to nearly 1 ìm). We performed MALDI-TOF, liquid chromatography/electrospray ionization mass spectrometry (LC/ESIMS), chemical activity tests, atomic force microscopy (AFM), and Fourier transform infrared (FTIR) spectroscopy experiments on the MAPLE-deposited films in order to characterize the chemical and physical integrity of the transferred biomolecular films. This manuscript also demonstrates the unique capabilities MAPLE possesses as a potential processing tool to fabricate microarrays and active elements for microfluidic sensors. We deposited adjacent arrays of two different biomaterials with pattern dimensions ranging from 20 to 250 ìm. Biomaterial and polymer multilayers were also deposited *in situ* as a method to retain these patterns during exposure to an aqueous environment. Overall, we find that MAPLE successfully forms thin films and patterns of unperturbed biomaterials that retain their chemical activity and singular mass identity.

Experimental Methods

Thin Film Depositions

The MAPLE process is used to form thin films in vacuum by exposing a frozen target of mixed volatility to a rastered excimer laser (20 ns, 193 nm) that is pulsed at 10 Hz. Figure 1 is a diagram of the MAPLE apparatus. The targets consist of a dilute mixture of biomolecules in an aqueous buffer solution (large solute molecules embedded in a volatile matrix). The target concentration can be altered from 10^{-2} to 10^{-4} g biomolecule/g buffer solution. Depending on the solute molecular weight, these concentrations translate to a water molecule-to-biomolecule ratio of $3x10^4$ to $1x10^6$ for high and low solute concentrations in the matrix, respectively. The fluence of the UV laser can be varied from 0.1 to 1 J/cm^2, but fluences of less than 0.2 J/cm^2 were used to prevent damage to the deposited biomolecules. The rate of film growth can be changed over three orders of magnitude by adjusting the laser pulse frequency (1 to 20 Hz), the target-to-substrate distance (d = 3 to 7 cm where closer target-to-substrate distances, d, increase the deposition rate by roughly $1/d^2$), the laser fluence, the target temperature, or the macromolecular concentration in the matrix.

MAPLE is chosen to deposit biomaterials because it is able to transfer delicate polymeric materials undamaged.[37,38,39] The incident laser pulse used for MAPLE initiates a photothermal process in the water matrix, vaporizing the frozen material and releasing the biomaterial into the chamber. Because of the low concentration of biomaterial in the target, the photons interact primarily with the matrix, and the macromolecules are released intact and undamaged. The momentum, resulting from the vaporization process,

carries the water and biomaterials toward the substrate. Because water is volatile at ambient temperature, it is removed by the pumping system. The base pressure in the MAPLE chamber is 10^{-5} torr, and during depositions the pressure rises to no greater than 10^{-4} torr due to laser-induced desorption. We purposely perform the depositions under vacuum so that the more volatile matrix component (water) is pumped away, while the heavier, less volatile biomolecules condense on the substrate to form the desired film. This vaporization process is in contrast to traditional pulsed laser deposition (PLD) where the laser energy directly interacts with the molecules to be deposited.[40] Due to the destruction of chemical bonds during this direct laser-material interaction, the chemical identity of the transferred species is often lost, and the film is comprised of material with lower average molecular weight than the starting material.[41] The indirect manner in which the MAPLE process transfers energy to the macromolecules is key to the successful, non-destructive deposition of organic materials such as polymers and biomolecules.

MAPLE depositions are compatible with many different substrates such as polymers, ceramics, metals, and semiconductors. The current studies deposited physisorbed biomolecules on gold, platinum, NaCl plates, Si(111), hydrogenated Si, and ethylene vinyl acetate (EVA) coated Si. The choice of substrate is important for the biomolecule adhesion and is the subject of continued research by this group.

The composition and temperature of the MAPLE matrix are also important in determining the rate of deposition and structure of the biomolecule. We used a phosphate buffer solution (PBS) at pH 7.2, 300 mOsm for the horseradish peroxidase (HRP, Sigma Chemical Corp.) and insulin (Sigma Chemical Corp.) depositions. To form 20 to 250 ìm

diameter patterns of biomaterials, a 40 ìm thick, gold-plated nickel shadow mask from Metrographics (a Division of Dynamics Research Corporation) was attached directly to the substrate during the depositions. In order to increase the material adhesion and to aid in growing thicker films, a composite target of 1 wt% polyethylene glycol (PEG, MW = 4600 amu, Aldrich) and 0.5 wt% biomaterial was used. Specifically, a composite mixture of PEG and PBS was used for the shadow mask depositions of fluorescent-tagged dextran (MW = 10,000 amu, Molecular Probes) and HRP in order to deposit films thick enough for fluorescence to be optically observed in a dry environment. A liquid nitrogen-cooled cold finger controls the temperature of the matrix inside the deposition chamber. A matrix temperature of –60ºC resulted in the most uniform films and a high deposition rate, but depositions can be performed at temperatures ranging from –40 (higher growth rate) to –160ºC (lower growth rate).

Thin Film Characterization

To characterize the MAPLE-deposited protein thin films, we utilized MALDI, LC/ESIMS, FTIR, and chemical activity tests. For MALDI, the samples were reconstituted in 5 µL of 0.1% trifluoroacetic acid (TFA)/water and 1 µL of this solution were added to 4 µL of a sinapinic acid (SA, 3,5-Dimethoxy-4-hydroxycinnamic acid) matrix solution (saturated SA in 70% acetontrile/30% 0.1%TFA in water). The analyte/matrix solution was thoroughly mixed and 2 µL of this solution was deposited on a stainless steel probe tip. The sample was dried under a stream of air. MALDI analysis was performed using a linear time-of-flight mass spectrometer with a 1.5 m path length.[42] The acceleration voltage was 23 kV and a microchannel plate detector, operating at 1.8 kV, was used for ion detection. Signals were amplified with an EGG preamplifier and

collected with a LeCroy 9350A digitizing oscilloscope. Samples were desorbed with a LSI 337-ND nitrogen laser operating at 1-2 Hz. The pulse energy of the laser was controlled with a variable attenuator and the pulse energy was adjusted to the threshold energy necessary for desorption (< 10 μJ/pulse). A 25 cm focal length lens was used to focus the laser on the sample. The instrument was externally calibrated with Angiotensin I (M.W. 1295.6) and bovine insulin (M.W. 5733.6) before and after the samples were analyzed. There was no contamination from the insulin calibrant, as demonstrated by blank runs between sample and calibrant analyses.

For liquid chromatography/electrospray ionization mass spectrometry (LC/ESIMS) analysis, evaporated samples were reconstituted in approximately 20 μL of 0.1% TFA in water. Spectra were obtained on a Thermoquest-Finnigan LCQ ion trap mass spectrometer. The heated capillary temperature was set at 200 °C and the capillary and tube lens offsets were zero. The instrument was scanned from 700-2000 amu. The instrument was tuned and calibrated with a standard myoglobin tuning solution prior to use. Electrospray ions were generated with a home-built microspray interface, based on the design of Fales and coworkers consisting of a 1.5 cm long, 190 μm o.d., and 50 μm i.d. fused silica capillary.[43] The capillary was held in place using a metal liquid chromatography union, and the electrospray voltage (1.5-2.5 kV) was applied to the solution through contact with the electrified union. Samples were introduced by liquid chromatography, using methods similar to those described by Hunt and coworkers.[44] The outlet of a capillary liquid chromatography column was connected directly to the metal union. The column consisted of a 20 cm piece of 190 μm o.d., 100 μm i.d. fused silica capillary column packed with 5 μm C18 chromatography support (YMC, Inc.). Samples

were loaded onto the column in 0.1% TFA and eluted with a mobile phase consisting of 70% acetonitrile/30% 0.1%TFA at a flow rate of 1 µL/minute (supplied by an Applied Biosystems Dual Syringe Drive pump). Electrospray spectra were obtained over the course of the 30 min elution time.

Several other methods were also used to characterize the thin films deposited by MAPLE. Thin films of HRP were deposited onto NaCl plates by both MAPLE and spray-coating. A Nicolet FTIR spectrometer was then used to obtain transmission spectra from 400 to 4000 cm^{-1}. The chemical activity of MAPLE-deposited protein was also analyzed by exposing HRP thin films to a standard 3,3'-diaminobenzidine (DAB) solution and optically observing the reduction of DAB. Micrographs of fluorescing Texas Red-labeled dextran films were obtained using a Nikon optical microscope equipped with a mercury arc lamp filtered with a standard G-2A filter block with a 510-560 nm window and a 590 nm Band pass filter.

Results and Discussion

Surface Morphology

To examine the surface morphology of protein films formed by MAPLE, we grew horseradish peroxidase (HRP) films at different deposition rates between 0.02 nm/laser shot and 0.06 nm/laser shot. We investigate the surface morphology of HRP films because the chemical integrity of this protein is easily analyzed through FTIR and chemical activity measurements that are described below. Figure 2(a) shows a 3D AFM image of a 200 nm thick HRP film grown at approximately 0.02 nm/laser shot. The root mean square (RMS) roughness is 90 nm, and there are undulations with peak-to-valley

heights of 150 nm. Overall, the film coverage is uniform over an area of 100 ìm^2. Figure 2(b) shows an AFM image of a 700 nm HRP film that was grown at three times the rate as the film shown in panel (a). The RMS roughness is 200 nm for this film, and there are undulations with peak-to-valley heights of nearly 1 ìm.

MAPLE has the ability to control film thickness as well as film uniformity and roughness by increasing or decreasing the deposition rate. Higher growth rates usually produce rougher, less uniform films while slow rates increase film uniformity and can produce remarkably smooth films.[38,40] This control enables MAPLE to tailor the surface morphology of thin films for specific applications. For example, some chemical sensing devices based on surface acoustic wave resonators require very smooth and thin films in order to achieve faster response rates and higher analyte sensitivity.[37,38] Conversely, as a means to increase the surface area for analyte binding, some biosensor devices require thicker films that have high surface areas.[45,46] The rough protein films formed by MAPLE in these studies could potentially increase the detection capability of a coated device by increasing the active protein area exposed to the analyte. If smoother films are desired, the rate of growth could be slowed by over an order of magnitude by decreasing the biomaterial concentration in the matrix, lowering the incident energy, and cooling the matrix to lower temperatures. This versatility is an advantage of MAPLE over other coating techniques, i.e., its ability to control the surface morphology of a biomaterial film and tailor the surface properties to the requirements of a specific device.

Characterization of MAPLE-deposited Protein Thin Films

I. Fourier Transform Infrared (FTIR) Spectroscopy

Infrared spectroscopy is frequently used as a characterization tool for biomolecules, and it is an accepted technique to gain information about not only primary chemical structure but also secondary structure.[47,48,49] We compared the FTIR spectra of the native protein to the spectra of laser-deposited protein by coating HRP on NaCl plates with spin-coating and MAPLE, respectively. Figure 3(a) shows the entire FTIR spectra (700 to 3500 cm^{-1}) for both the spin-coated (dashed line) and MAPLE-deposited (solid line) films. Both spectra are nearly identical over the entire spectral range, except for a atmospheric CO_2 peak in the spin-coated film. Specifically, the bands of amide I at 1650 cm^{-1} (C=O stretching), amide II at 1550 cm^{-1} (N-H deformation and C-N stretching), and three peaks below 1200 cm^{-1} (symmetric and asymmetric organic hydroxyl stretching) are well reproduced in the spectrum of the MAPLE-deposited film.

Information pertaining to secondary structure can also be obtained by analyzing slight shifts in the amide I and amide II peaks.[48,49] Upon denaturation of an á-helix, the amide I band shifts from 1650 cm^{-1} to 1640 cm^{-1}, while the amide II band shifts from 1550 cm^{-1} to higher frequencies. Figure 3(b) expands the frequency axis of the FTIR spectra for both the spin-coated and MAPLE-deposited films. There is clearly no shift from 1550 cm^{-1} in the amide II band of both spectra, while the amide I band for the MAPLE HRP film shows some broadening and a slight shift to higher frequencies. The peak maximum for the amide I band for the MAPLE film, however, remains at 1650 cm^{-1}. This peak at 1650 cm^{-1} suggests that the majority of á-helix structures remain intact, but the broadening and slight shift to higher frequencies may be evidence that some á-helix structures change to random coil structures. Overall, it appears that the

laser-matrix interaction and vapor deposition during MAPLE does not significantly alter the secondary structure of transferred HRP.

II. MALDI-TOF and LC/EIMS Analysis

We performed both MALDI and LC/EIMS experiments on MAPLE-deposited insulin (a molecular weight standard for MALDI experiments) in order to determine whether the laser-matrix interaction alters the parent mass of the transferred protein. Both MALDI and electrospray analysis confirmed the presence of intact insulin in MAPLE-deposited films. The MALDI spectrum is shown in Figure 4a. The spectrum is characterized by a number of peaks at lower molecular weight that can be attributed to the laser desorption of salts and the organic matrix used to facilitate MALDI analysis. Although the masses of these peaks are not labeled in the figure, they include such ions as m/z 23 and m/z 39 (Na^+ and K^+, respectively), as well as peaks attributable to matrix, such as $[M+H]^+$, $[2M+H]^+$, or other adducts of matrix and matrix fragments for sinapinic acid (e.g., m/z 225, 451). These lower molecular weight peaks are typically observed in MALDI spectra. The spectrum above m/z 600 is relatively clean. A major peak is observed at m/z 5734, corresponding to the protonated molecular ion $[M+H]^+$ for insulin. A smaller satellite peak corresponds to an adduct ion between insulin and a matrix molecule $[M+SA+H]^+$. The only other significant peak in the spectrum arises from the doubly charged insulin ion, which appears at m/z 2867 and is characteristic of MALDI spectra of insulin.

The spectrum shown here demonstrates that a majority of the insulin molecules are deposited intact on the Si surface. The mass of the major peak in the spectrum (m/z =

5734) correlates well with the expected mass, within the mass accuracy of this system (0.1%). The measurement is not sufficiently accurate to confirm that small changes in mass (e.g. alterations to the molecule) have not occurred. However, the absence of significant ion abundances between the matrix region and the molecular ion region of the spectrum indicates that no degradation products of significant mass and abundance are observed. However, the data cannot rule out the possibility that some of the insulin molecules may be significantly decomposed into relatively small fragments of low abundance. It would not be possible to easily confirm their presence in the MALDI spectrum, due to the large number of low molecular weight peaks in the mass spectrum that result from matrix related species.

In order to obtain further information about possible alterations of the insulin molecule during the MAPLE process, the extracted samples were also analyzed by LC/ESIMS. When analyzed using a C18 microcapillary column, the sample yields a single chromatographic peak. The LC/ESI mass spectrum in obtained from that peak is shown in Figure 4(b). The electrospray spectrum is characterized by two major peaks, which occur at m/z 1434.6 and m/z 1912.1. These two major ion peaks arise from multiply-charged ions that are formed from insulin. The peak at m/z 1434.6 corresponds to the $[M+4H]^{4+}$ ion, while the peak at m/z 1912.1 corresponds to the $[M+3H]^{3+}$ ion. The molecular weights calculated from these peaks are 5734.4 and 5733.3, respectively. These values are within 0.02% of the expected average molecular weight (5733.6) and indicate that no substantial modification of the insulin has occurred. For example, insulin consists of an A and B chain that are linked by disulfide bonds, and the B chain contains an additional intrachain disulfide bond. The calculated molecular weight indicates that

none of these bonds have been reduced during the MAPLE process. The LC/ESI MS results also suggest that there is no significant degradation of the insulin molecule. Only one chromatographic peak is observed, indicating that no single degradation product is present in significant abundance. However, this does not eliminate the possibility that many fragments of low abundance (and consequently not observed) are formed. Future analytical studies will focus on better establishing the absence of degradation products.

III. Protein Activity Analysis

In order to further test the chemical and physical integrity of MAPLE-transferred protein, we determined whether the MAPLE process inhibited the ability of HRP to catalyze the reduction of 3,3'-diaminobenzidine (DAB). Figure 5(a-b) shows optical micrographs of two MAPLE-deposited HRP films on glass slides (thickness = 500 and 10 nm, respectively) after 20 min of H_2O_2/DAB exposure. Both films clearly show areas that are dominated by a dark brown precipitate characteristic of reduced DAB. The images also show that the drop of test solution dissolved the majority of HRP and carried both the protein and the reduced DAB to the edge of the drop. This results in a non-uniform coating and a concentrated line of reduced DAB at the solvent front. The appearance of a dark-colored precipitate, however, is a clear indication that the protein transferred by MAPLE maintains its activity after laser-exposure and vacuum deposition. The 500 nm HRP film produced more precipitate than the thinner film, but the 10 nm protein film, which contains no more than a few monolayers of HRP, still produced visible amounts of reduced DAB.

The DAB results prove that MAPLE-transferred HRP retain their structure near the active catalytic site during the laser-matrix interaction, desorption, and deposition process. After exposure to the test solution, the 10 nm HRP film also had a visually observable and consistent amount of reduced DAB over the entire test droplet/HRP interface. This result implies that MAPLE forms a film of active HRP and that the percentage of molecules transferred to the film undamaged is high.

The lower portion of both panels (a) and (b) in Figure 5 show the area of the films where the deposited HRP was washed away by the droplet of test solution, while the top shows the unperturbed HRP film. Upon exposure to the test droplet, the protein was lifted into solution because the HRP is weakly bound (physisorbed) on the glass substrate. As discussed below, we are able to deposit a semi-permeable polyurethane membrane that shields the underlying protein from the aqueous test solution and eliminates this solvation effect.

Thin Film Structures Deposited by MAPLE

I. Patterns and Multilayers

MAPLE is capable of forming mesoscopic patterns of biomolecules by placing a shadow mask on the substrate that receives the vapor-deposited material. A mask fabricated by Dynamics Research Corporation was used in conjunction with MAPLE to form patterns of an HRP/ polyethylene glycol (PEG) composite on a hydrogenated silicon substrate. We found that depositing a protein-polymer composite enhanced adhesion to the hydrogenated silicon substrate and enhanced edge resolution for depositions through

the shadow mask. However, this composite was still susceptible to an aqueous environment, and H_2O_2/DAB exposure washed the HRP/PEG pattern from the substrate.

In an attempt to retain active biomaterial patterns after exposure to an aqueous environment, we deposited an array pattern of HRP spots coated with a semi-permeable polymer membrane.[50,51,52] We deposited the HRP/PEG composite pattern by MAPLE followed by PLD deposition of a polyurethane (PU) film over the entire substrate. PLD was chosen to deposit the PU film because of previous experiments that successfully formed thick (several ìm), semi-permeable PU membranes for analytical applications.[53] We find that the PLD-deposited PU overcoat is water repellant, protects both the protein and PEG pattern during H_2O_2/DAB exposure, and forms a membrane with pores large enough to allow analyte molecules to penetrate the film (see DAB exposure results below).

Figure 6 shows optical micrographs of this multilayer structure formed from the sequential deposition of patterned HRP/PEG composite and PU by MAPLE and PLD, respectively. Figure 6(a) shows one part of the patterned film with an array of 250 ìm diameter HRP/PEG dots. The entire patterned film includes different areas of lines and dots with diameters ranging from 250 to 20 ìm. The HRP/PEG film is 500 nm thick while the polyurethane overcoat is nearly 2 ìm thick. The micrograph in panel (a) was taken prior to H_2O_2/DAB exposure in order to demonstrate the appearance of the protein/polymer multilayer before the precipitation of reduced DAB occurred. The HRP/PEG film appears rough with small light brown particulates. The rough nature of the HRP/PEG film shown in Figure 6 is most likely due to the addition of PEG to the protein target. When fast deposition rates are used to grow PEG films, we find that both

PLD and MAPLE form films with high concentrations of particlates.[41] The amount of particulates depends on the PEG molecular weight, target concentration, and laser fluence, and current investigations are aimed at improving PEG film quality. Another goal of our current research in this area is to find better composite materials or surface interactions to improve adhesion without disrupting film quality or pattern integrity. The array pattern, however, can easily be distinguished in the current experiment, and the areas of protein are clearly defined from the areas with no sensitive material.

Panels (b-d) of Figure 6 are higher magnification micrographs of the protein/polymer multilayer *after* H_2O_2/DAB exposure. Panels (b-d) show three DAB-exposed HRP patterns: (b) a 250 ìm dia dot, (c) a 250 ìm dia line, and (d) a 50 ìm dia dot. The dotted line in panel (d) is shown as an aid to the viewer and is an outline of deposited protein pattern. The slightly lighter color inside the line is due to the deposited HRP, but the small diameter of this dot and the small color change for regions containing protein make it difficult to discern the pattern boundary. In stark contrast to Figure 5 where the test droplet completely dissolved the HRP film and left a circular ring of precipitate, the micrographs in Figure 6 show that the protein patterns remain unperturbed after exposure to the DAB solution. Each panel also shows that the reduced DAB is present after exposure to the test droplet, demonstrating active HRP is present in the film. Instead of the precipitate being carried to the edge of the test droplet, as is the case for the uncoated HRP film, the dark brown precipitate is now confined to the areas on the film where the active protein is present. Even the 50 ìm diameter dot shown in panel (d) contains substantial dark brown precipitate. The 20 ìm diameter dot array (not shown), however, did not show consistent activity. This is most likely due to the random

distribution of pores in the PU overcoat and does not indicate that 20 ìm patterns of active proteins cannot be formed using this technique. These figures demonstrate that MAPLE is able to deposit biomaterial and polymer multilayers and form stable 50 ìm resolution patterns (1960 ìm^2) of sensitive material that survive exposure to analyte solutions.

II. Multi-material Arrays

Fabrication of biosensor arrays and antibody or DNA microarrays require multiple materials to be patterned adjacently on the same substrate. By simply changing the target material and adjusting the shadow mask, MAPLE is capable of forming adjacent patterns of many different materials. Figure 7 shows two different adjacent patterns of HRP and fluorescent-tagged dextran (10,000 MW, Texas Red tag) formed by MAPLE depositions through a shadow mask. Both depositions were performed using a composite matrix of buffer solution, PEG, and HRP or dextran. PEG composites were deposited to enhance film adhesion and to aid in growing thick dextran films necessary to produce sufficient red fluorescence emission in a dry environment that could be observed by the CCD camera attached to the microscope. Panel (a) shows a white light optical micrograph of adjacent 50 ìm diameter dots of HRP and dextran, while panel (b) shows neighboring 50 ìm wide lines of HRP (perpendicular line) and dextran (parallel lines). To demonstrate that these patterns are two adjacent materials, we exposed both films to a black light. Panels (c) and (d) show UV-exposed micrographs of the films shown in panels (a) and (b), respectively. Both sets of dextran patterns fluoresce due to the

attached Texas Red tag, while the HRP pattern remains dark because the protein is not fluorescent-tagged.

Figures 6 and 7 demonstrate that by forming patterns of adjacent materials and multilayer films, MAPLE and PLD are capable of sequentially depositing multiple active elements by simply changing the target and adjusting the shadow mask. We have shown that MAPLE is able to deposit thin films of active biological materials, while PLD successfully deposits protective overcoat films. These results, in combination with known PLD capabilities to deposit electronic materials, show that laser-based tools are capable of fabricating entire miniature sensing devices or microarrays with active elements on the order of tens of ìm.

Summary and Future Work

We have shown that thin films and patterns of several biomaterials can be deposited by a psuedo-dry technique termed matrix assisted pulsed laser evaporation (MAPLE). MALDI-TOF and LC/ESIMS analysis of MAPLE-deposited material demonstrate that this laser-based approach forms thin films of biomaterials by carrying intact biomolecules from target to substrate. Infrared spectra of HRP films show that the chemical and physical structure of the protein is maintained post-MAPLE transfer. A solvent-phase activity test performed on HRP films also indicates that the majority of transferred protein retains chemical and physical structure. These results are the first demonstration that pure films of intact, active biomolecules can be deposited using a vapor-deposition technique.

The results presented in this paper highlight several attributes MAPLE has for depositing biomaterial thin films. MAPLE is capable of forming thin films over a wide range of thicknesses from 10 nm to over 1 ìm and with accurate thickness control (<0.05 nm/laser shot). Many current technologies using SAMs are only capable of depositing monolayers, while other thick film deposition techniques, such as ink jet printing, are unable to control thickness and film uniformity. MAPLE's thickness control and accurate material placement, therefore, may be particularly useful for thick film amperometric biosensors where accurate thickness control and uniform film coverage are crucial to signal output.[54] The surface morphology of biomaterial films can also be controlled by MAPLE, enabling this technique to tune the roughness of films to meet specific device requirements. Multilayers of many different materials (i.e., polymers, active biomolecules) can also be formed *in situ*, enabling protective overcoats or membranes to be easily formed. By using MAPLE and PLD together, laser-based techniques could sequentially deposit electrodes, active biological molecules, and a polymer or biomaterial coating to immobilize and protect the underlying materials. Multiple materials can also be patterned adjacently on the same substrate, enabling microarrays to be fabricated with feature size and spacing as small as 20 ìm. MAPLE is unique because it is able to combine these attributes into one processing tool to fabricate structures unattainable by other technologies.

The experiments described here demonstrate that MAPLE is an excellent method to deposit biomaterial thin films. Due to this success, we plan to continue our basic and applied research in this area. Current studies are focused on applying MAPLE to biomolecules that are used in biosensors with the goal of fabricating a functioning

microfluidic device. We also plan to explore the extent to which MAPLE can be used to transfer different biomolecules such as DNA or antibodies. The current studies also highlight the need for further investigations to determine the best methods to adhere MAPLE-deposited biomolecules to different surfaces without perturbing their activity. Our current efforts to create a polymer-protein composite to increase adhesion were successful, but patterning this composite material produced particulate-rich films. We therefore are exploring methods to modify the substrate surface to increase material adhesion as well as methods to chemically immobilize deposited molecules *in situ.* MAPLE also holds potential to deposit not only biomolecules but also a matrix that acts to maintain the activity of the sensitive material or help adhere it to the substrate. Overall, MAPLE holds promise as a novel and versatile technique to deposit and pattern thin, active biomolecular films of varying thickness and surface morphologies.

Figure Captions

1) Schematic of MAPLE apparatus. A low-fluence UV laser pulse is focused on a frozen target consisting of a dilute mixture of biomaterial in an aqueous buffer solution. The laser energy is absorbed by the matrix (water molecules), resulting in desorption of both water and biomolecules. The more volatile water is pumped away by the vacuum, and the less volatile biomaterial is captured by the substrate, forming a pure film of active material.

2) AFM images of two HRP films: (a) 200 nm thick HRP, (b) 600 nm thick HRP. The images demonstrate how MAPLE is able to control film thickness and surface morphology.

3) FTIR spectra of spin-coated and MAPLE-deposited HRP films. (a) MAPLE film reproduces the native protein spectrum over the entire spectral range. (b) The amine I and II peaks for the MAPLE spectrum show no significant shifts, implying the protein structure is intact post-transfer.

4) (a) MALDI-TOF spectrum of MAPLE-deposited insulin (peaks due to matrix materials are off scale). Single peak suggests that the majority of insulin transferred by MAPLE retains a singular mass. (b) LC/ESIMS spectrum of MAPLE-deposited insulin also suggests that MAPLE does not damage the protein during transfer.

5) (a) 500 nm and (b) 10 nm HRP film grown by MAPLE. Micrograph was taken after exposure to DAB solution. Dark brown color indicates the transferred HRP retains its ability to catalyze the reduction of DAB.

6) (a) 250 ìm HRP/PEG dot array with polyurethane (PU) overcoat before exposure to aqueous DAB exposure. (b) 250 ìm HRP dot with PU over-layer post-DAB exposure. (c)

250 ìm HRP line with PU over-layer post-DAB exposure. (d) 50 ìm HRP dot with PU over-layer post-DAB exposure. The PU overcoat confines the active signal (brown precipitate) within the HRP domains.

7) (a) White light micrograph of a 50 ìm HRP/PEG dot array adjacent to fluorescently-tagged dextran array. (b) White light micrograph of a 50 ìm HRP/PEG line perpendicular to a dextran line. (c) UV-exposed dot array. (d) UV-exposed perpendicular lines.

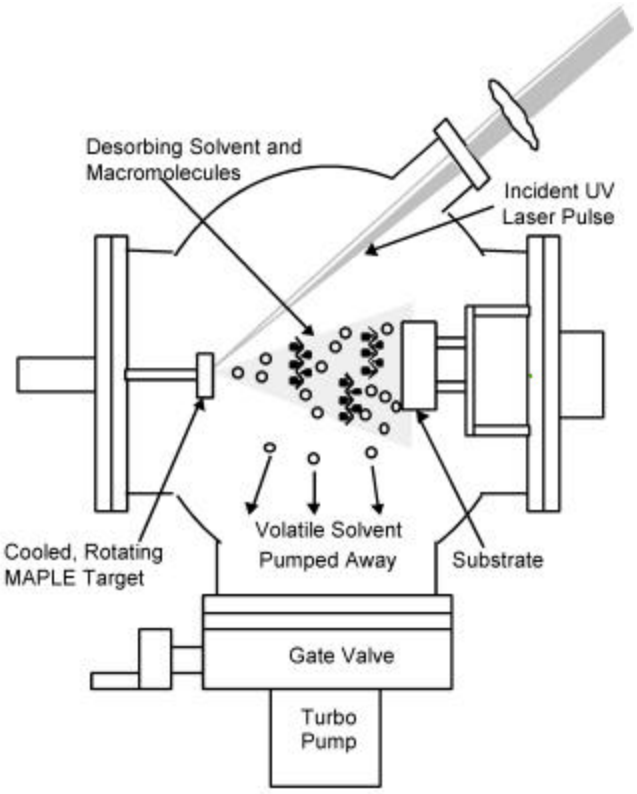
Desorbing Solvent and
Macromolecules
Incident UV
Laser Pulse
Cooled, Rotating
MAPLE Target
Volatile Solvent
Pumped Away
Substrate
Gate Valve
Turbo
Pump

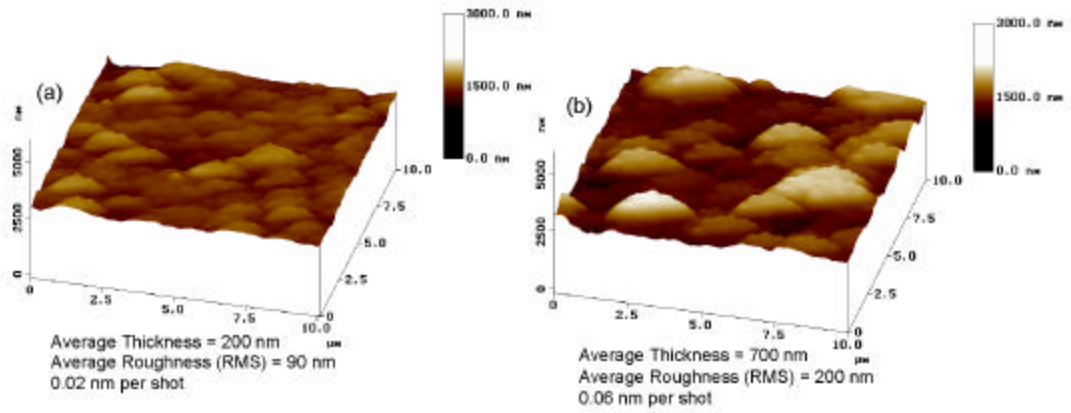
(a)
3000.0 nm
1500.0 nm
0.0 nm
5000
2500
0
0
2.5
5.0
7.5
10.0
μm
Average Thickness = 200 nm
Average Roughness (RMS) = 90 nm
0.02 nm per shot
(b)
3000.0 nm
1500.0 nm
0.0 nm
5000
2500
0
0
2.5
5.0
7.5
10.0
μm
Average Thickness = 700 nm
Average Roughness (RMS) = 200 nm
0.06 nm per shot

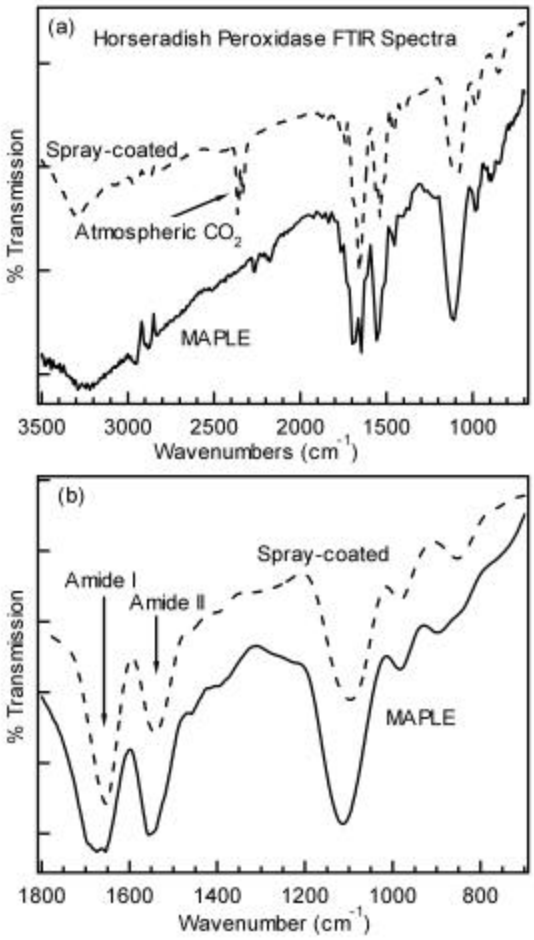
(a)
Horseradish Peroxidase FTIR Spectra
Spray-coated
Atmospheric CO_2
MAPLE
% Transmission
3500
3000
2500
2000
1500
1000
Wavenumbers (cm^{-1})
(b)
Amide I
Amide II
Spray-coated
MAPLE
% Transmission
1800
1600
1400
1200
1000
800
Wavenumber (cm^{-1})

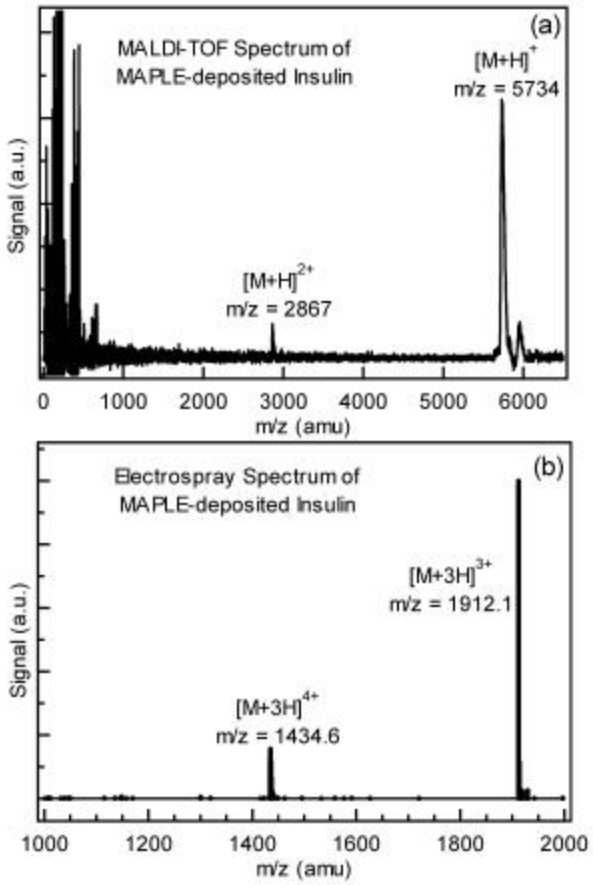
(a)
MALDI-TOF Spectrum of
MAPLE-deposited Insulin
[M+H]+
m/z = 5734
[M+H]2+
m/z = 2867
Signal (a.u.)
0
1000
2000
3000
4000
5000
6000
m/z (amu)
(b)
Electrospray Spectrum of
MAPLE-deposited Insulin
[M+3H]3+
m/z = 1912.1
[M+3H]4+
m/z = 1434.6
Signal (a.u.)
1000
1200
1400
1600
1800
2000
m/z (amu)

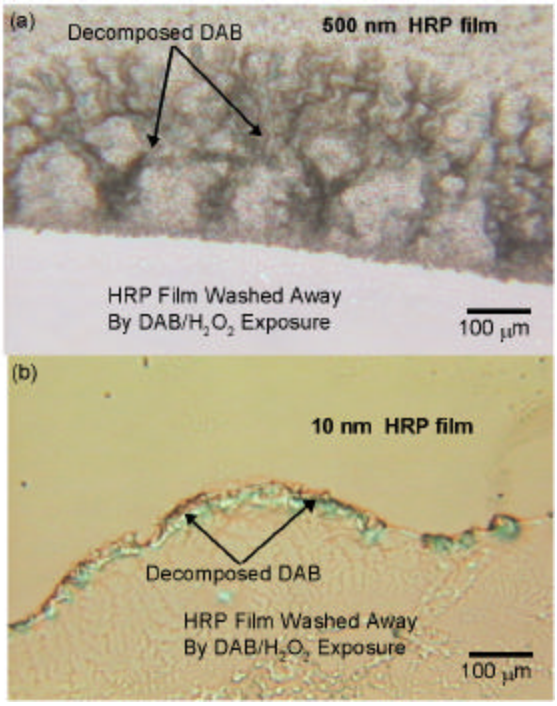
(a)
Decomposed DAB
500 nm HRP film
HRP Film Washed Away
By DAB/H2O2 Exposure
100 μm
(b)
10 nm HRP film
Decomposed DAB
HRP Film Washed Away
By DAB/H2O2 Exposure
100 μm

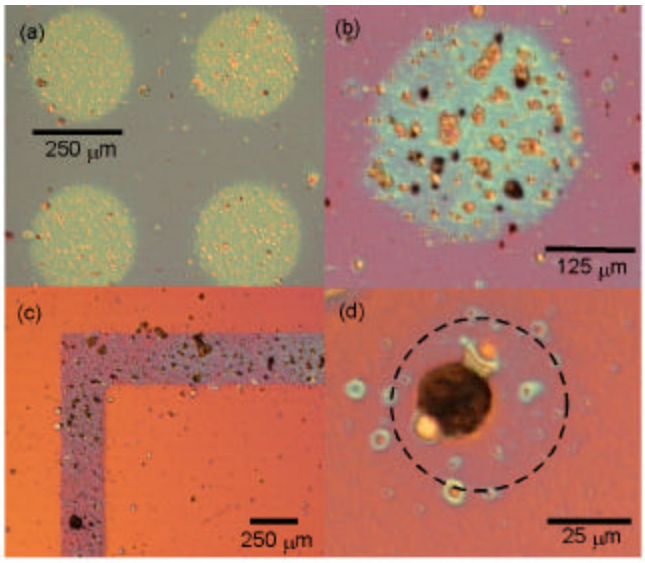
(a)
250 μm
(b)
125 μm
(c)
250 μm
(d)
25 μm

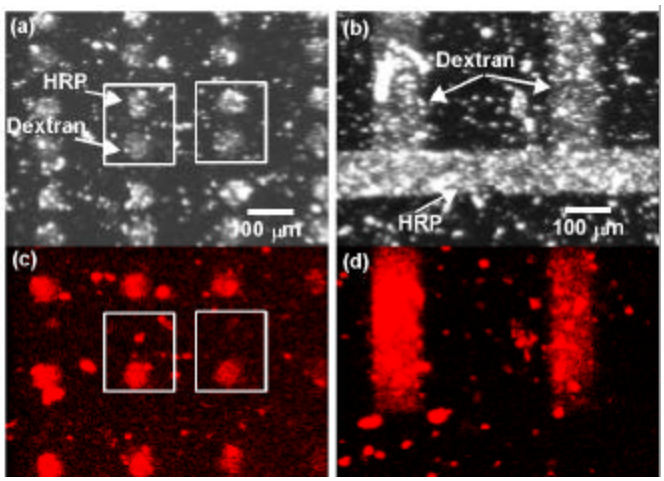
(a)
HRP
Dextran
100 μm
(b)
Dextran
HRP
100 μm
(c)
(d)

[1] Kane, R. S.; Takayama, S.; Ostuni, E.; Ingber, D. E.; Whitesides, G. M. *Biomaterials* **1999**, *20*, 2363.
[2] Brooks, S. A.; Dontha, N.; Davis, C. B., Stuart, J. K., O'Neill, G.; Kuhr, W. G. *Anal. Chem.* **2000**, *72*, 3253.
[3] Zhang, S.; Wright, G.; Yang, Y. *Biosens. Bioelectron.* **2000**, *15*, 273.
[4] Yershov, G.; Barsky, V.; Belgovskiy, A.; Kirillov, E.; Kreindlin, E.; Ivanov, I.; Parinov, S.; Guschin, D.; Drobishev, A.; Dubiley, S.; Mirzabekov, A. *Proc. Nat. Acad. Sci. USA* **1996**, *93*, 4913.
[5] Guschin, D.; Yershov, G.; Zaslavsky, A.; Gemmell, A.; Shick, V.; Proudnikov, D.; Arenkov, P.; Mirzabekov, A. *Anal. Biochem.* **1997**, *250*, 203.
[6] Graves, D. J.; Su, H. J.; McKenzie, S. E.; Surrey, S.; Fortina, P. *Anal. Chem.* **1998**, *70*, 5085.
[7] Miyachi, H.; Hiratsuka, A.; Ikebukuro, K.; Yano, K.; Muguruma, H.; Karube, I. *Biotech. Bioeng.* **2000**, *69*, 323.
[8] Borman, S. *Chem. Eng. News* **2000**, *78*, 31.
[9] Wisniewski, N.; Reichert, M. *Coll. Surf. B* **2000**, *18*, 197.
[10] Chuard, C.; Vaudaux, P.; Waldvogel, F. A.; Lew, D. P. *Antimicrob. Agents Chemother.* **1993**, *37*, 625.
[11] Price, J. S.; Tencer, A. F.; Arm, D. M.; Bohach, G. A. *J. Biomed. Mater. Res.* **1996**, *30*, 281.
[12] Calhoun, J. H.; Mader, J. T. *Clin. Orthop.* **1997**, 206.
[13] Zdrahala, R. J.; Zdrahala I. J. *J. Biomater. Appl.* **1999**, *14*, 67.
[14] Sun, S.; Ho-Si, P.; Harrison, D. J. *Langmuir* **1991**, *7*, 727.
[15] Fujiwara, I.; Ohnishi, M.; Seto, J. *Langmuir* **1992**, *8*, 2219.
[16] Vaidya, R.; Tender, L. M.; Bradley, G.; O'Brien II, M. J.; Cone, M.; Lopez, G. P. *Biotechnol. Prog.* **1998**, *14*, 371.
[17] Sirkar, K.; Revzin, A.; Pishko, M. V. *Anal. Chem.* **2000**, *72*, 2930.
[18] Li, T.; Mitsuishi, M.; Miyashita, T. *Chem. Lett.* **2000**, 608.
[19] Xia, Y. N.; Whitesides, G. M. *Ann. Rev. Mat. Sci*.**1998**, *28*, 153.
[20] Lahiri, J.; Ostuni, E.; Whitesides, G. M. *Langmuir* **1999**, *15*, 2055.
[21] Bernard, A.; Delamarche, E.; Schmid, H.; Michel, B.; Bosshard, H. R.; Biebuyck, H. *Langmuir* **1998**, *14*, 2225.
[22] James, C. D.; Davis, R. C.; Kam, L.; Craighead, H. G.; Isaacson, M.; Turner, J. N.; Shain, W. *Langmuir***1998**, *14*, 741.
[23] Delamarch, E.; Bernard, A.; Schmid, H.; Michel, B.; Biebuyck, H. *Science* **1997**, *276*, 779.
[24] Delamarch, E.; Bernard, A.; Schmid, H.; Bietsch, A.; Michel, B.; Biebuyck, H. *J. Am. Chem. Soc.* **1998**, *120*, 500.
[25] Patel, N.; Sanders, G. H. W.; Shakesheff, K. M.; Cannizzaro, S. M.; Davies, M. C.; Langer, R.; Roberts, C. J.; Tendler, S. J. B.; Williams, P. M. *Langmuir* **1999**, *15*, 7252.
[26] Folch, A.; Toner, M. *Biotech. Prog.* **1998**, *14*, 388.
[27] Kimura, J.; Kawana, Y.; Kuriyama, T. *Biosensors* **1988**, *4*, 41.
[28] Newman, J. D.; Turner, A. P. F. *Anal. Chim. Acta* **1992**, *262*, 13.
[29] Roda, A.; Guardigli, M.; Russo, C.; Pasini, P.; Baraldini, M. *BioTechniques* **2000**, *28*, 492.
[30] Odde, D. J.; Renn, M. J. *Trends Biotechnol.* **1999**, *17*, 385.
[31] Odde, D. J.; Renn, M. J. *Biotechnol. Bioeng.* **2000**, *67*, 312.
[32] Chrisey, D.; Piqué, A.; Fitz-Gerald, J.; Ringeisen, B.; Modi, R. *Laser Focus World* **2000**, 36, 113.
[33] Nelson, R. W.; Thomas, R. M.; Williams, P. *Rapid Commun. Mass. Sp.*, ***1990***, *4*, *348*.
[34] Tsuboi, Y.; Goto, M.; Itaya, A. *Chem. Lett.* **1998**, 521.
[35] Phadke, R. S.; Agarwal, G. *Mat. Sci. Eng. C* **1998**, *5*, 237.
[36] Agarwal, G.; Phadke, R. S. *Nanotech.* **1999**, *10*, 336.
[37] McGill, R. A.; Chung, R. Chrisey, D. B.; Dorsey, P. C.; Matthews, P.; Piqué, A.; Mlsna, T. E.; Stepnowski, J. I. *IEEE Trans. Ultrason. Ferr.* **1998**, *45*, 1370.
[38] McGill, R. A.; Chrisey, D. B.; Piqué, A.; Mlsna, T. E. *Proc. SPIE Laser Applications in Microelectronic and Optoelectronic Manufacturing III*, **1998**, 255.
[39] Piqué, A.; McGill, R. A.; Chrisey, D. B.; Leonhardt, D.; Mslna, T. E.; Spargo, B. J.; Callahan, J.H.; Vachet, R. W.; Chung, R.; Bucaro, M. A. *Thin Solid Films* **1999**, *356*, 536.
[40] *Pulsed Laser Deposition*. Chrisey, D. B., Hubler, G. K., Eds.; Wiley: New York, 1994.

[41] Bubb, D. M.; Ringeisen, B. R.; Callahan, J. H.; Horwitz, J. S.; McGill, R. A.; Houser, E. J.; Chrisey, D. B., unpublished results.
[42] Tang, X. D.; Callahan, J. H.; Zhou, P.; Vertes, A. *Anal. Chem.* **1995**, *67*, 4542.
[43] Konig, S.; Fales, H. M. *Anal. Chem.* **1998**, *70*, 4453.
[44] Cox, A. L.; Skipper, J.; Chen, Y; Henderson, R. A.; Darrow, T. L.; Shabanowitz, J.; Englehard,V. H.; Hunt, D. F.; Slinguff, C. L. *Science* **1994**, *264*, 716.
[45] Mulchandani, A.; Mulchandani, P.; Chen, W.; Wang, J.; Chen, L. *Anal. Chem.* **1999**, *71*, 2246.
[46] Albareda-Sirvent, M.; Merkoçi, A.; Alegret, S. *Sensors and Actuators B* **2000**, *69*, 153.
[47] Chittur, K. K. *Biomaterials* **1998**, *19*, 357.
[48] Kumar, C. V.; Chaudhari, A. *J. Am. Chem. Soc.* **2000**, *122*, 830.
[49] Panick, G.; Winter, R. *Biochem.* **2000**, *39*, 1862
[50] Newman, J. D.; White, S. F.; Tothill, I. E.; Turner, A. P. F. *Anal. Chem.* **1995**, *67*, 4594.
[51] Teoh, S. H.; Tang, Z. G.; Ramakrishna, S. *J. Mat. Sci.: Mat. Med.* **1999**, *10*, 343.
[52] Zhang, S.; Zhao, H.; John, R. *Anal. Chim. Acta* **2000**, *421*, 175.
[53] Bubb, D. M.; Ringeisen, B. R.; Horwitz, J. S.; Piqué, A.; McGill, R. A.; Chrisey, D. B., unpublished results.
[54] Gooding, J. J; Hall, E. A. H.; Hibbert, D. B. *Electroanal.* **1998**, 10, 1130.